Title

THE EFFECT OF RETAINED AUSTENITE ON THE CRYOGENIC MECHANICAL PROPERTIES IN FINE-GRAINED Fe-12Ni-0.25Ti ALLOY

Author

Hwang, Sun-Keun.

Publication Date

1974-12-01

LBL-3503
c. 1

THE EFFECT OF RETAINED AUSTENITE ON THE CRYOGENIC MECHANICAL PROPERTIES IN FINE-GRAINED Fe-12Ni-0.25Ti ALLOY

Sun-Keun Hwang
(M.S. thesis)

December, 1974

Prepared for the U. S. Atomic Energy Commission
under Contract W-7405-ENG-48

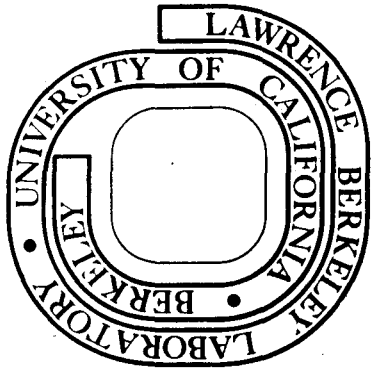

LBL-3503

DISCLAIMER

THE EFFECT OF RETAINED AUSTENITE ON THE CRYOGENIC MECHANICAL PROPERTIES IN FINE-GRAINED Fe-12Ni-0.25Ti ALLOY

Contents

THE EFFECT OF RETAINED AUSTENITE ON THE CRYOGENIC MECHANICAL PROPERTIES IN FINE-GRAINED Fe-12Ni-0.25Ti ALLOY

Sun-Keun Hwang

Inorganic Materials Research Division, Lawrence Berkeley Laboratory and Department of Materials Science and Engineering, College of Engineering University of California, Berkeley, California

ABSTRACT

The phenomenological behavior of diffusion-controlled reverted austenite in a fine-grained Fe-12Ni-0.25Ti cryogenic alloy system was investigated. The grain-refined martensite structure was exposed to a temperature within two-phase ($\alpha + \gamma$) region. The stability of equilibrium austenite was affected by the decomposition temperature. It appeared to be the redistribution of solute elements that controlled the stability. The microstructural appearance of retained austenite was examined using transmission electron microscopy. A preferential distribution of the austenite phase along the martensite lath boundaries was observed. A precipitate-correlated austenite nucleation was also found to occur. The beneficial effect of the introducing retained austenite appeared not only in the tensile elongation but also in the Charpy impact toughness at low temperatures. A degradation in the yield stress occurred after an extended holding at an intermediate temperature or after a moderate time holding at a relatively high temperature. The deterioration of strength was interpreted in terms of retained austenite stability and precipitate overaging. The retained austenite did not improve K_{IC} at 77°K. Unstable crack propagation developed during the fracture toughness tests of most specimens containing retained austenite phase.

I. INTRODUCTION

The development of the retained austenite phase in ferritic steels has been a stimulating research subject in past years. The importance of this phenomenon lies, in the first place, in the unusual type of phase transformation. Secondly, the mechanical properties are significantly affected by the presence of the retained austenite although not in an obvious manner.

Concerning the stability of austenite phase, there have been two groups of experimental observations:

1) Stabilized austenite due to the lattice distortion induced by the martensitic transformation of surrounding materials.[1]
2) Chemically stabilized austenite by a compositional change in a local area.[3-7]

Kelly and Nutting[1] attributed the stability of partially transformed austenite to difficulties in the cooperative movement of atoms to form martensite. Austenite enriched with certain alloying elements which lower Ms (Martensite transformation starting temperature) can be chemically stabilized. In an Fe-Ni based alloy, the Ms is chiefly affected by the amount of the solute elements.[8-9] When a metastable martensite is exposed to an elevated temperature within two phase (austenite + ferrite) range austenite of high Ni concentration precipitates by a diffusion-controlled equilibrium decomposition.[10] This "reversion" reaction takes place over a wide range of temperatures including overaging temperatures of maraging steels[3-5] as well as tempering temperatures in low-nickel cryogenic steels.[6-7] As a consequence it is usually associated with the partitioning of other solute elements: Mo and Ti in the overaged particles of maraging steels, C

in the carbide particles in low-nickel steels. The reverted austenite produced in this manner is so enriched in solute atoms that it is extremely persistent against subsequent transformation. Besides the above two mechanisms Leslie and Miller[2] reported the effect of ultra-fine austenite grain size on the austenite stability.

Although there have been numerous reports on the mechanical properties of ferritic steels with some volume fraction of retained austenite, the exact role of it is not unequivocal. The bulk of prior research on the maraging steels[5,11,12,16] suggests a deleterious effect of retained austenite on the strength. In spite of these observations Peters[13,14] found a continuously increasing hardness along with an appreciable stable austenite formation. A similar tendency was later observed by Pampillo and Paxton.[19] The enhancement of tensile elongation, on the other hand, has been shown.[4,18,19] A good combination of strength and ductility, if a proper amount of retained austenite is controlled, was suggested to solve engineering problems such as forming or machining process.[4] The beneficial effect of retained austenite is most striking in tempered, low-nickel cryogenic steels.[6-7] The ductile-brittle transition temperature is significantly lowered by introducing a fine-structured retained austenite through a tempering process.

Recently a grain-refining technique, utilizing an alternate thermal-cycling process, has been developed for the Fe-12Ni-0.25Ti cryogenic alloy system.[21] The alloy, after grain-refined (about 1μ), showed an extraordinary amount of plasticity in low temperature (77°K, 4°K) fracture toughness tests without sacrificing yield strength. As a part of the continuing program, the behavior of the retained austenite

introduced in this ductile matrix was investigated in the present study. Facilitated by the enormously large grain boundary area, stable austenite can form easily. In this context, a somewhat elaborate thermal-cycling process to achieve fine-grained structure was performed.

The investigation was undertaken firstly to examine the morphology and stability of the retained austenite. Nextly, the cryogenic mechanical properties were studied after introducing a certain amount of retained austenite. The work was then extended to the Fe-8Ni-2Mn-0.25Ti system.

II. EXPERIMENTAL PROCEDURE

A. Material Preparation and Initial Processing

Low carbon alloys of nominal composition Fe-12 Ni-0.25Ti were induction melted in an argon gas atmosphere then cast into 9.1 Kg ingots in a copper chill mold. The ingots were homogenized under vacuum at 1150°C for 80 hours. Then these were up-set cross forged at 1100°C into 1.3 cm thick by 10.2 cm wide plates and 1.9 cm thick by 6.4 cm wide plates respectively to meet later specimen dimensions. The plates were annealed at 900°C for two hours under argon gas atmosphere to remove prior deformation strain, then air cooled to room temperature. Each plate was cut into several blocks and grain-refined through the thermal-cycling procedure described elsewhere.[21] A schematic diagram of the heat-treatment for grain refining is shown in Figure 1. The result of chemical analysis on two randomly chosen ingots is presented in Table I.

B. X-Ray Diffraction Analysis

Specimens, 2 cm by 3 cm wide and 0.5 cm thick were cut along the longitudinal direction of the plates. To remove any mechanically-induced transformation effect the surface preparation was carefully conducted. Pre-polishing was done by step-by-step hand grinding using emery paper up to 600 grade. Then chemical polishing was carried out using the solution, 100 ml H_2O_2 + 3 ml HF. The final polishing was done on 1μ polishing cloth. X-ray diffraction on these surface-treated specimens was carried out using Cu-Kα radiation with LiF monochrometer. The calculation of the retained austenite volume percent was based on Miller's method,[22,23] comparing average integrated intensities of the

(220) and (311) austenite peaks to that of the (211) martensite peak. No correction was made to take the precipitate into account. Also, a preferred orientation which might set in during a heat treatment was not considered to be so serious in the averaged intensities.

C. Optical and Electron Microscopy

Specimens for metallographic study were cut from bulk material, usually from Charpy bars or fracture toughness specimens which had been tested at 77°K. The specimens were etched with 5% Nital for optical microscopy. For transmission electron microscopy (TEM) thin sheets were cut along transverse direction. Chemical thinning was conducted in the solution; 100 ml H_2O + 4 ml HF. Thin foils were made by a jet-polishing technique using a standard solution (75 g CrO_3 + 800 ml CH_3COOH + 21 ml H_2O) under 20∿30 V. The electron-microscopes used were mainly a Hitachi HU-125 operated at 100 kV and a Siemens Elmiscope 1 operated at 100 kV. The fracture surfaces of Charpy specimens tested at 77°K were examined in a JEOLCO JSM-U_3 scanning electron microscope operated at 25 kV.

D. Mechanical Testing

Cylindrical tensile specimens of 12.7 mm gage length and 3 mm gage diameter were machined from the blanks. The rolling direction of the plate was kept consistent with the axial loading direction of the specimen. Tensile tests were conducted in liquid nitrogen (77°K) and liquid helium (4°K) respectively using an Instron machine equipped with suitable cryostats. A strain rate of 0.04/min. was employed. When there was no clear yield point the yield stress was calculated by the 0.2% offset method. When a sharp yield point appeared the yield stress was taken as the upper yield point. The total elongation was determined by

measuring the distance between gage length markings before and after testing. A traveling microscope with an accuracy of ±0.01 mm was used for the measurements. The uniform elongation was determined from the chart by comparing the total elongation calculated from the chart with the value actually measured on the specimens.

Charpy V-notched specimens of standard ASTM size were machined from the material blanks. The direction of the length was kept consistent with the rolling direction, thus the loading direction was perpendicular to it. Charpy impact tests at 77°K were carried out as described in ASTM E23-72. Tests at temperature near 4°K were conducted using the sample insulating technique developed by Jin, et al.[24]

Compact tension specimens for fracture toughness tests were machined from the blanks keeping the longitudinal direction consistent with the loading direction. Since the thickness required by ASTM E399-72 was not available (more than 6 cm) a reduced thickness of 1.8 cm was used. Then equivalent K_{IC} values were calculated by methods based on the "Equivalent energy" and "J-Integral" concepts.[25] The fracture toughness tests were conducted at 77°K on a MTS universal testing machine equipped with a liquid nitrogen cryostat.

III. RESULTS

A. Microstructures

1. Grain-Refined Structure

As shown in Figure 1, the heat treatment employed in this experiment consisted of two parts. The first part is the grain refining through alternate thermal cycling: 730°C/2 hours/AC (air cooling to room temperature) + 650°C/2 hours/AC, two cycles. The second part is the reheating treatment at various temperatures within two phase range. An optical micrograph taken from the grain-refined specimen (Figure 2(a)) shows an average grain size of about 1μ. TEM pictures of the same structure are shown in Figure 3(a) and (b). A typical martensite lath structure with tangled dislocations is shown in Figure 3(a). In some areas (Figure 3(b)) precipitates which presumably formed during heating were observed. This grain-refined structure is regarded as a standard structure of the starting material for the later study on retained austenite.

2. Morphology of Retained Austenite

A reheating treatment, 550°C/8 hours/WC (Water cooling to room temperature), apparently does not affect the grain size (Figure 2(b)). TEM micrographs (Figure 4) revealed plate-like precipitates lying along the <110> directions of the matrix. These precipitates are tentatively determined as Ni_3Ti in light of extensive data in precipitation studies in maraging steel.[28] A dark-field technique was used to view the retained austenite after the reheating treatment. A diffraction pattern which is close to a ring pattern was obtained from a very fine-grained region

(Figure 5). The compositions of the equilibrium phases at 550°C consist of approximately Fe-23.5%Ni austenite and Fe-5%Ni. Therefore lattice parameters for these phases were taken as $(a_0)_\gamma = 3.573\text{Å}$ and $(a_0)_\alpha = 2.869\text{Å}$ respectively.[26] Comparison between the calculated r values and the measured ones showed excellent agreement (Table II). Dark-field micrographs were obtained from $\{200\}_\gamma$ spots to illuminate retained austenite. The selected area diffraction pattern with its analysis and the corresponding BF (bright-field), DF (dark-field) pictures are shown in Figure 6 to Figure 9. Figure 6 and Figure 7 were taken from a specimen heat treated 525°C/1 hour/WC, while Figure 8 was obtained after 550°C/8 hours/WC treatment. Shown in Figure 9 is a picture taken from a Fe-8Ni-2Mn-0.25Ti alloy processed through a similar heat treatment. The morphology of the retained austenite is seen in most cases to be elongated particles along martensite lath boundaries. The details will be discussed later.

B. Measurement of Retained Austenite

Effectively, no retained austenite was resolved in the grain-refined structure. The variation in the volume percent of retained austenite after a number of selected heat treatments is shown in Figure 10. The amount of stable austenite which is retained at room temperature increases with holding time at low temperatures (525°C ∿ 575°C). The reverse is true at high temperature (600°C). The absolute amount of retained austenite in this experiment, however, may not be valid considering the error range (up to 3%) in an X-ray measurement. Since 550°C appeared to be the optimum temperature, data were obtained for isothermal holding at 550°C. Plotted in Figure 11 is the volume percent retained austenite vs.

logarithmic scale of holding time (hours). An almost linear slope is observed. Stability at 77°K was tested through 4 hours immersion in liquid nitrogen. The result, illustrated by the open circles in Figure 11, shows about the same stability of retained austenite at 77°K. After very long holding, however, a slight decrease in the stability at 77°K occurred. Actually, the retained austenite after 550°C/2 hours/WC was proved to be stable even at 4°K. The stability with respect to the mechanical deformation was examined by performing a cold rolling at room temperature. After 50% reduction in thickness the result shows almost complete martensitic transformation.

C. Mechanical Properties at Low Temperatures

1. Tensile Properties

The tensile properties at 77°K after reheating for 2 hours at various temperatures are plotted in Figure 12. Compared to that of initial grain-refined material, the yield stress increases slightly after low temperature (475°C) reheating. However, it decreased as the reheating temperature was raised (600°C). On the whole, the total and uniform elongations increased evenly. Typical engineering stress-strain curves are shown in Figure 13. The slope of the curve within the small strain range becomes steeper and a sharp yield point appears as the reheating temperature is lowered. An improvement in the elongation was also observed at 4°K. The engineering stress-strain curves at 4°K are shown in Figure 14.

2. Charpy Impact Energy

The absorption energy in Charpy impact tests at both 77°K and 4°K was markedly increased after reheating treatments. The increment ranged from 30 to 60 ft-lbs., depending on the particular ingot. The results of the 77°K tests are plotted in Figure 15, where the reheating temperature is taken as a variable. The C_v (absorption energy in Charpy V-notched impact test) values for the 8-hour treatment is generally higher than those for the 2-hour treatment. However, after the 600°C treatment the C_v's for the two different holding times fall at the same level within a scattering band. After the 475°C treatment the increment is low compared to the others. Plotted in Figure 16 are C_v values at 77°K after isothermal treatment at 550°C. Again C_v with holding time tends to increase, but not in a strong manner. A plot of C_v data at 4°K after 2 hours reheating treatment at different temperatures is shown in Figure 17. An increment ranging from 30 ft-lbs. to 40 ft-lbs. is evident compared to the untreated grain-refined structure. The effect of cooling rate after a final heat treatment was examined using different cooling media. As shown in Table IV, the cooling rate turned out to be insignificant with the exception of a furnace cooling after the grain-refinement. The C_v at 77°K was dropped by 25 ft-lbs. in the furnace cooling compared to the air cooling.

The fracture surfaces of Charpy bars tested at 77°K are shown in Figure 18. Both grain-refined and reheated (550°C/8 hours/WC) structures exhibit the characteristic mode of void nucleation and coalescence which is regarded[18,21] as a typical failure mechanism in this ductile alloy system.

3. Fracture Toughness

The equivalent K_{IC} values measured at 77°k are presented in Table V. As mentioned earlier, the values are calculated by the "Equivalent energy" and "J-Integral" approaches, which show excellent agreement in static (Cross Head Speed.; 1.3 cm × 10^{-3}/sec.) tests. Despite the improvements in the tensile elongation and the Charpy impact energy, the low-temperature fracture toughness was not improved by the reheating treatments. The 550°C/2 hours/WC treatment maintains about the same K_{IC}. In other treatments K_{IC} is generally lowered. The degradation appears in another aspect, a mode of crack propagation.

Unstable crack propagation developed in most specimens which had been reheat treated. A typical load-COD curve is shown in Figure 19.

IV. DISCUSSION

A. Morphology and Stability of Retained Austenite

Effectively no retained austenite was identified in the grain-refined structure by either X-ray diffraction analysis or TEM work. Therefore the austenite stabilization mechanism claimed by Kelly and Nutting[1] must be rare in this Fe-12Ni-0.25Ti system. Then the stability of reverted austenite produced by reheating to a temperature within the two phase region can be attributed to a partitioning of solute atoms[3-7] and/or to a grain size effect.[2] The grain size effect is considered first. Leslie and Miller[2] observed an increasing amount of retained austenite in very fine-grained low carbon Fe-Ni steels annealed at a relatively low temperature in the two phase region. They suggested an unfavorable growth of martensite platelets in the ultra-fine prior austenite grains. The grain size effect appears to be real in the present system, for retained austenite was not observed in a coarse-grained (40∿50μ) alloy of the identical composition, treated with a similar reheating.[27] Nevertheless, the experimental results in the current investigation could not be interpreted solely in terms of an ultra-fine grain size, based on the following discussion. The diffusion-controlled austenite reversion is thermally activated. The rate of reaction and the amount of product austenite phase should increase on raising the temperature or extending the holding time. If the grain size alone were the governing factor on the stability of the reverted austenite we should have a larger amount of retained austenite after holding at a higher temperature. On the contrary, as shown in Figure 10, amount of retained austenite after the 600°C treatment is less than that produced

by the 550°C treatment. Furthermore the amount of retained austenite after the 600°C treatment decreases as the holding time increases. Since we observed little grain growth even with a 650°C/2 hours/AC treatment (final treatment of the grain-refining process (Figure 2(a)), grain growth is not likely to occur during the treatment 600°C/2 hours/WC. Then the decrease in retained austenite after a high temperature anneal ought to be due to some other mechanism than the simple grain size effect. As has been discussed in a number of reports on similar systems,[3-7] subtle movement of solute atoms seems to participate in the austenite stabilization. At a relatively low temperature, the reverted austenite should have a comparatively high Ni concentration, as predicted by the equilibrium phase diagram. Depending on the reaction temperature and heating rate, Ni_3Ti precipitation is advanced or overlapped with the formation of equilibrium austenite. Ni_3Ti precipitates will eventually suffer overaging at a temperature higher than the optimum aging temperature ($\sim$475°C) or at a relatively low temperature with extended holding. If some dissolution of overaged Ni_3Ti precipitates into the reverted austenite occurs[5] this austenite would be enriched in Ni and Ti. Considering that these elements lower M_s significantly,[9] the austenite enriched in them is expected to remain untransformed on a subsequent cooling to room temperature. The Ni concentration of the equilibrium austenite decreases as the temperature becomes higher. At the same time the relative amount of equilibrium austenite increases considerably by the lever rule. As a matter of course, Ti, if taken from the overaged precipitates, adjusts towards an uniform distribution over the austenite grains. The resulting individual austenite grain is depleted in Ni and Ti,

and hence has a relatively high M_s. This appears to be the reason why there is less retained austenite after a relatively high temperature reheating treatment. Once the reverted austenite is stabilized at a moderate temperature it hardly loses its stability against thermal treatment such as quenching to a sub-zero temperature. This was confirmed by immersing the same specimen in liquid nitrogen and liquid helium.

However, the retained austenite may not exhibit the consistent stability against mechanical deformation. Although a good deal of information is available about the plastically-induced transformation in metastable austenitic steel,[29] there have been few reports on the stability of retained austenite against plastic deformation in ferritic steel.[18] In the present study of 50% reduction in thickness by a cold rolling resulted in almost complete transformation of austenite to martensite (Figure 11). More discussion on this will be done in the next section.

Since the time Floreen and Decker[16] observed a retained austenite distribution along martensite platelet boundaries in a 18Ni maraging steel, corroborative observations have accumulated.[14,17,19] Intermetallic compound precipitates also have been suggested to motivate austenite nucleation[5,6,18] but direct observation was not available. In the present study TEM work gave some support to this hypothesis. In the first place, the r measurement on the diffraction pattern (Figure 5) allows us to discern the diffraction spots caused by the f.c.c. retained austenite phase. The dark-field micrographs obtained from these spots show that the retained austenite lies primarily along martensite lath

boundaries (Figure 6) and sub-grain boundaries (Figure 9). From the analysis of a diffraction pattern (Figure 8) the orientation relationship was observed to follow closely that of Kurdjumov-Sachs,[31] viz, $(111)_\alpha // (110)_\gamma$; $[\bar{1}10]_\alpha // [\bar{1}1\bar{1}]_\gamma$. In some other instances (Figures 6 and 9) it is interesting to note an orientation relationship $(311)_\alpha // (310)_\gamma$; $[\bar{1}21]_\alpha // [\bar{1}3\bar{1}]_\gamma$. The reverted austenite nucleated on the precipitates can be seen by careful examination of Figure 7, which was taken from the specimens reheated for 1 hour at 525°C. Recognizing that the temperature employed is higher than the optimum aging temperature it is not surprising to see austenite reversion accompanied by precipitate dissolution.

B. Mechanical Properties

1. Tensile Properties

A direct loss of strength proportional to the amount of retained austenite has been reported in many research works.[5,11,12,16] Certain of the results remain controversial.[13,14,19] A positive contribution of retained austenite to the yield stress was suggested,[19] i.e., when austenite is retained, martensite lath boundaries may cause difficulties in transmitting slip across these boundaries.

From the results obtained in the present alloy at 77°K (Figure 12), the variation in the yield stress and elongation may be considered as follows. Either a recovery effect or the retained austenite phase, per se, might be regarded as responsible for the degradation in the yield stress after the relatively high temperature treatment. However, if the recovery effect were taken alone, it would not account for the evenly increased elongation after the 475°C treatment. It is not unreasonable

to expect that the strength of the martensite matrix would be lost by the replacement of b.c.c. phase with f.c.c. phase. However, with a small amount of retained austenite, the yield stress after the 550°C treatment stays about the same as that of the initial grain-refined material. Besides, the yield stress after 600°C treatment is less than that after the 550°C treatment while the reverse was observed about the amount of retained austenite (Figure 10). Therefore it appears that the stability rather than the amount (within small extent) of retained austenite affects strength. The following explanation is suggested. As the reheating temperature is raised, precipitates which contributed to the yield stress overage. At the same time, the degradation in the stability of the retained austenite accelerates early yielding by permitting a stress-induced martensitic transformation.[29] Additionally the recovery process may aggrevate the situation. A set of engineering stress-strain curves shown in Figure 13 support the above explanation. The appearance of a sharp yield point in 475°C treatment reflects the precipitate effect. The slope of the curve is smoothened by the early yielding after a high temperature treatment.

An increase in elongation with increasing retained austenite content has been reported in several systems.[4,18-20] In recent work on maraging steel[19] the uniform elongation was observed to increase by about 4% for 150 hours aging followed by rapid initial increase. In the present investigation the uniform and total elongations rapidly increased, then stayed roughly constant irrespective of the heating temperature. Actually the increment in the tensile elongation turned out to be a simple reflection of the increment in the uniform elongation.

The reduction in area, on the other hand, was not affected much although the initiation of necking was delayed by the increase in the uniform elongation.

2. Charpy Impact Toughness (C_v)

The role of retained austenite in surpressing the ductile-brittle transition temperature in 9Ni and 6Ni steels has been described as a "sink effect"[6] or "Shock absorber effect."[20] The f.c.c. austenite has both higher solubility for common impurities and more potential slip systems than the b.c.c. martensite has. High solubility is beneficial to dissolve impurities especially when they segregate along grain boundaries. The variety of slip system accelerates cross-slip and tends to increase the amount of plastic deformation prior to failure.

The appreciable increase in C_v at both 77°K and 4°K after reheating treatment can be attributed to the existence of retained austenite. The lower increment after the 475°C treatment compared to the others (Figure 15) should be attributed to the precipitate effect discussed in the previous section. The ductile-brittle transition temperature of the present alloy is already lower than 77°K after grain refining. Therefore the role of retained austenite in the present improvement of C_v is not due to surpressing the transition temperature. The rapid increase in C_v together with the rapid increase in elongation imply a significant improvement of matrix or grain boundary properties.

Fractographs taken from the fracture surface of Charpy bars tested at 77°K (Figure 18) tell that retained austenite does not give rise to an apparent change in the mode of failure, micro-void nucleation and coalescence.

3. Fracture Toughness

There have been few reports on the effect of retained austenite on the low temperature K_{IC} (equivalent) value. As a matter of fact some improvement in K_{IC} would be expected on introducing a tough austenite phase. This expectation could be strongly inferred from the tensile test and the Charpy impact test results. Nevertheless, reheating treatments turned out to be ineffective in further improving the K_{IC} values of the previously ductile matrix. It appears that the transition temperature in K_{IC} test is changed by the reheating treatment. At the same level of K_{IC} a deterioration appears in the development of unstable crack propagation. Although the reason is not quite clear at the moment one speculation is that martensite transformation occurs ahead of crack tip during the fatiguing process. The preferential distribution of retained austenite along martensite lath boundaries has been confirmed in the previous microstructural studies. If stress or strain induced transformation occurs, prior grain boundaries or lath boundaries will contain newly formed martensite. This fresh martensite might give rise to a local stress concentration, facilitating unstable crack propagation. One critical difference between the Charpy test and usual (static) fracture toughness test is the strain rate. Therefore a 10^3 times faster cross head speed was employed to examine the strain rate effect. Although K_{IC} calculations based on two different approaches (Table V) showed significant discrepancies, the comparative values were not improved by the reheating treatment.

V. CONCLUSIONS

Based on the present study on the retained austenite phase in a fine-grained Fe-12Ni-0.25Ti alloy, the following conclusions are made:

1) The diffusion-controlled reverted austenite can be chemically stabilized. The local redistribution of solute atoms appears to be responsible for the decreased stability at a relatively high temperature.

2) The distribution of retained austenite takes place predominantly along martensite lath boundaries. Precipitate-correlated austenite nucleation was also observed.

3) Most of austenite chemically stabilized by the reheating process is unstable against mechanical deformation.

4) The presence of retained austenite contributes an improvement in low-temperature elongation and Charpy impact energy.

5) The reheating treatment does not improve low-temperature fracture toughness in the present ductile alloy system. Unstable crack propagation is, in fact, pronounced after the reheating treatment.

VI. RECOMMENDATIONS FOR FUTURE WORK

When the amount and the stability of diffusion controlled equilibrium austenite is controlled properly, the technique is promising for improvement of low temperature ductility. Future investigations should delineate the behavior of retained austenite in fatigue pre-cracked fracture toughness test. It may require extensive microstructural study on the fractured region. Employing the technique to introduce retained austenite the following considerations are recommended:

1) Optimum temperature within two phase range should be determined by dilatometry in version of chemical stabilization of reverted austenite.
2) Preparation of active nucleation sites for reversion reaction should be advanced. These might be either fine-grained structure or various precipitates which contain strong austenite stabilizer.
3) Possible negative contribution due to mechanically induced transformation ought to be taken into account.

ACKNOWLEDGEMENTS

The author is indebted to Professor J. W. Morris, Jr. for his extensive guidance and encouragement throughout this study. Special appreciation is extended to Dr. Sungho Jin for helpful discussion and continuous encouragement.

This research was supported by the Office of Naval Research under contract N00014-69-A-1062, NR 031-762, and by the Atomic Energy Commission through the Inorganic Materials Research Division of the Lawrence Berkeley Laboratory.

REFERENCES

1. P. M. Kelly and J. Nutting, J. of the Iron and Steel Inst. 197, 199 (1961).
2. W. C. Leslie and R. L. Miller, Trans. ASM 57, 972 (1964).
3. S. Floreen, Met. Rev. 126, 115 (1968).
4. P. Legendre, Cobalt 29, 171 (Dec. 1965).
5. A. Goldberg, Trans. ASM 61, 26 (1968).
6. C. W. Marschall, R. F. Heheman and A. R. Troiano, Trans. ASM 55, 135 (1962).
7. S. Nagashima, et al., Trans. ISIJ 11, 402 (1971).
8. W. S. Owen, E. A. Wilson and T. Bell, High Strength Materials, V. F. Zackay, Editor (John Wiley & Sons, Inc., 1965), p. 167.
9. R. B. G. Yeo, Trans AIME 227, 884 (1963).
10. N. P. Allen and C. C. Early, J. of the Iron and Steel Inst., 281 (Dec. 1950).
11. R. F. Decker, NPL Symposium No. 15, Teddington, England, The Relation Between the Structure and Mechanical Properties of Metals (1963).
12. A. M. Hall, NASA SP-5051, Battele Memorial Inst. (1968).
13. D. T. Peters and C. R. Cupp, Trans. AIME, 236, 1420 (1966).
14. D. T. Peters, Trans. ASM 61, 63 (1968).
15. R. L. Miller, Met. Trans. 3, 905 (1972).
16. S. Floreen and R. F. Decker, Trans. ASM 55, 518 (1962).
17. H. Haga, Trans. ISIJ 13, 141 (1973).
18. S. D. Antolovich, A. Saxena and G. R. Chanani, Met. Trans. 5, 623 (1974).

19. C. A. Pampillo and H. W. Paxton, Met. Trans. 3, 2895 (1972).

20. S. Yano, et al., Trans. ISIJ 13, 133 (1973).

21. S. Jin, J. W. Morris, Jr. and V. F. Zackay, Met. Trans, to be published.

22. R. L. Miller, Trans. ASM 57, 892 (1964).

23. R. L. Miller, Trans. ASM 61, 592 (1968).

24. S. Jin, W. A. Horwood, J. W. Morris, Jr. and V. F. Zackay, Advances in Cryogenic Engineering 19, 373 (1974).

25. P. C. Ricardella and J. L. Swedlow, HSST Tech. Rep. No. 33, under ONR subcontract No. 3196 (Oct. 1973).

26. E. A. Owen, et al., Proc. Phys. Soc. (London) 49, 315 (1937).

27. S. Jin, S. K. Hwang, and J. W. Morris, Jr., to be published.

28. C. P. Miller and W. I. Mitchell, J. Iron and Steel Inst. 203, 899 (1965).

29. D. Fahr, Met. Trans. 2, 1883 (1971).

30. C. Crussard, et al., Trans. ASM 55, 1021 (1962).

31. G. Thomas, I-Lin Cheng and J. R. Mihalisin, Trans. ASM 62, 852 (1969).

Table I. Chemical composition of steel (wt %).

Ingot No.	Fe	Ni	Ti	C	N	O	P	S
7312-5	Bal.	11.99	0.20	0.005	<0.001	<0.001	0.001	0.002
745-12	Bal.	12.07	0.18	0.005	0.002	<0.001	0.001	0.002

Table II. Comparison of calculated r values to those Measured from Figure 5 on the film (unit: cm).

Phase / hkl	α'		γ	
	Calculated	Measured	Calculated	Measured
110	1.64	1.65		
111			1.61	1.65
200	2.32	2.37	1.86	1.88
211	2.84	2.81		
220	3.28	3.30	2.64	2.69
310	3.67	3.67		
311			3.09	3.10
322	4.02	4.00	3.23	3.15
321	4.35	4.40		
400	4.64	4.70	3.73	
331			4.06	

Lattice Parameter used for calculation[26]

α (Fe-5%Ni) : 2.869 Å

γ (Fe-24%Ni) : 3.573 Å

Camera Constant: 3.33 Å-cm

Table III. Tensile properties at low temperature.

at 77°K

H.T.	Y.S.(Ksi)	T.S.(Ksi)	T.E.(%)	U.E.(%)	R.A.(%)
G.R.	136.5	150.4	27.8	7.8	75.7
G.R.+475°C/2 hr/WC	139.2	146.4	32.2	13.2	75.6
G.R.+475°C/20hr/WC	142.5	148.9	31.2	13.4	75.0
G.R.+550°C/1 hr/WC	135.3	150.7	33.4	13.9	74.5
G.R.+550°C/2 hr/WC	135.2	152.7	32.6	13.1	74.8
G.R.+550°C/8 hr/WC	131.2	155.7	32.9	13.8	73.8
G.R.+550°C/60hr/WC	113.0	147.4	32.5	16.2	73.3
G.R.+600°C/2 hr/WC	122.5	141.4	32.6	12.9	77.9

at 4°K

H.T.	Y.S.(Ksi)	T.E.(%)	R.A.(%)
G.R.	187.3	18.7	62.6
G.R.+550°C/1 hr/WC	192.0	22.4	64.1
G.R.+550°C/2 hr/WC	176.0	23.9	63.8

G.R.: Grain-refining through thermal cycling (Figure 1)

T.E.: Total Elongation

U.E.: Uniform Elongation

Table IV. C_v values with varying cooling rate tested at 77°K (Unit: ft-lb)

Cooling Rate / H.T.	F.C.	A.C.	W.C.	I.B.Q.
G.R.	97.2	123.4	115.7	130.6
450°C/20 hrs	123.7	139.9	157.5	125.0
550°C/2 hrs	145.8	137.4	160.9	150.6

F.C.: Furnace cooling

A.C.: Air cooling

W.C.: Water cooling

I.B.Q.: Ice brine quenching

Table V. Fracture toughness at 77°K

C.H.S.: 1.3 cm × 10^{-3}/sec

units; ksi $\sqrt{in}$

H.T. \ Equivalent K_{IC}	From E.E.	From J-Int.
G.R.	298	300
G.R.+450°C/20hrs/WC	230	232
G.R.+475°C/2 hrs/WC	258	258
G.R.+550°C/2 hrs/WC	300	304
G.R.+550°C/60hrs/WC	280	281
G.R.+600°C/2 hrs/WC	274	274

C.H.S.: 1.3 cm/sec

H.T. \ K_{IC}	From E.E.	From J-Int.
G.R.	154	255
G.R.+550°C/2 hrs/IBQ	162	242
G.R.+550°C/2 hrs/AC	157	248

E.E.: Equivalent energy approach

J-Int.: J-Integral approach

C.H.S.: Cross Head Speed

FIGURE CAPTIONS

Figure 1. Schematic diagram of heat treatment.

Figure 2. Optical Micrographs

(a) grain-refined structure

(b) 550°C/8 hrs/WC after grain refining.

Figure 3. TEM micrographs of grain-refined structure

(a) typical martensite lath structure

(b) local area where precipitates exist.

Figure 4. TEM micrographs after 550°C/8 hrs/WC treatment.

Figure 5. Diffraction pattern close to ring pattern (after 550°C/8 hrs/WC).

Figure 6. TEM micrographs after 525°C/1 hr/WC treatment

(a) selected area diffraction pattern (SAD)

(b) bright-field micrograph (BF)

(c) dark-field micrograph obtained from $(200)_\gamma$ (DF) illuminating lath-boundary distribution of retained austenite.

Figure 7. Same specimen used in Figure 6, but different area

(a) SAD

(b) BF

(c) DF taken from $(200)_\gamma$ illuminating precipitates correlated retained austenite distribution.

Figure 8. TEM micrographs after 550°C/2 hrs/treatment

(a) SAD with analysis close to K-S relationship

(b) BF

(c) DF taken from $(200)_\gamma$.

Figure 9. TEM micrographs of Fe-8Ni-2Mn-0.25Ti alloy (600°C/2 hrs/WC after grain-refining)

(a) SAD

(b) BF

(c) DF taken from $(200)_{\gamma}$.

Figure 10. Volume percent retained austenite after reheating at various temperatures and holding time.

Figure 11. Stability of austenite after isothermal holding at 550°C.

Figure 12. Tensile properties at 77°K after reheating for 2 hours at indicated temperatures.

Figure 13. Stress-strain curves at 77°K tensile test.

Figure 14. Stress-strain curves at 4°K tensile test.

Figure 15. Increase in Charpy absorption energy at 77°K.

Figure 16. Variation in C_v at 77°K with isothermal holding at 550°C.

Figure 17. C_v at 4°K vs. reheating temperature.

Figure 18. Fractographs taken from tested (77°K) Charpy bars

(a) after grain-refined

(b) after 550°C/8 hrs/WC treatment following grain refinement.

Figure 19. Load-COD curves in K_{IC} test at 77°K.

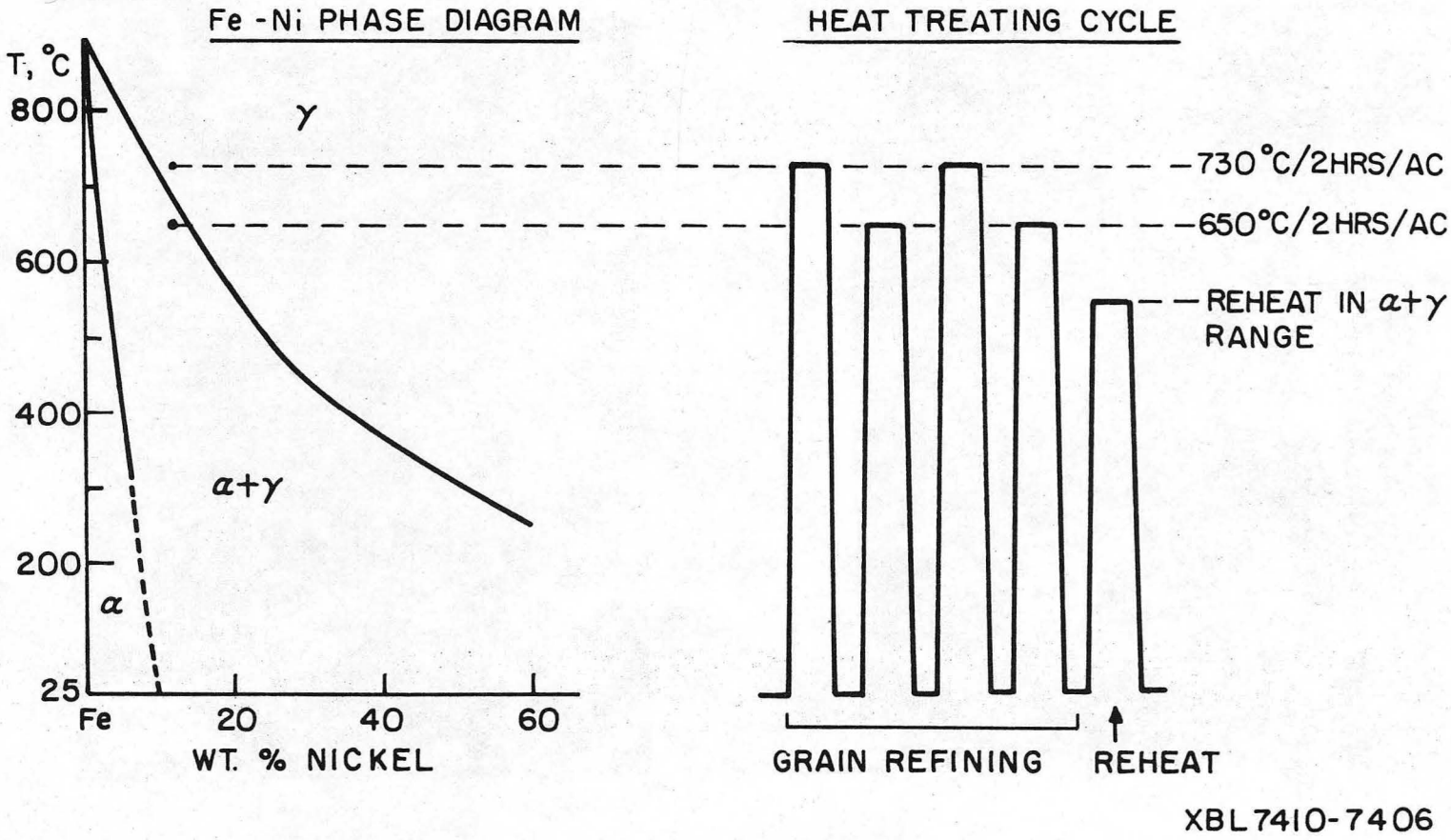

Fig. 1

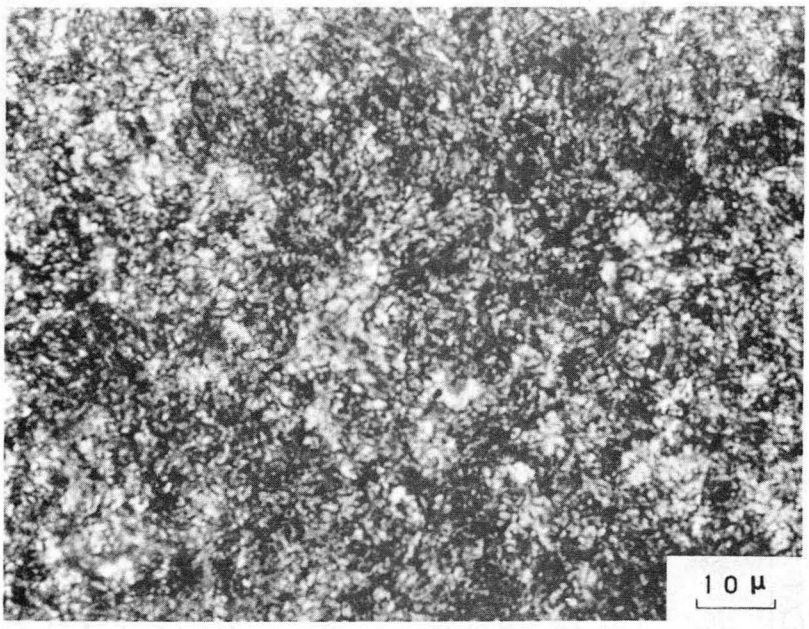

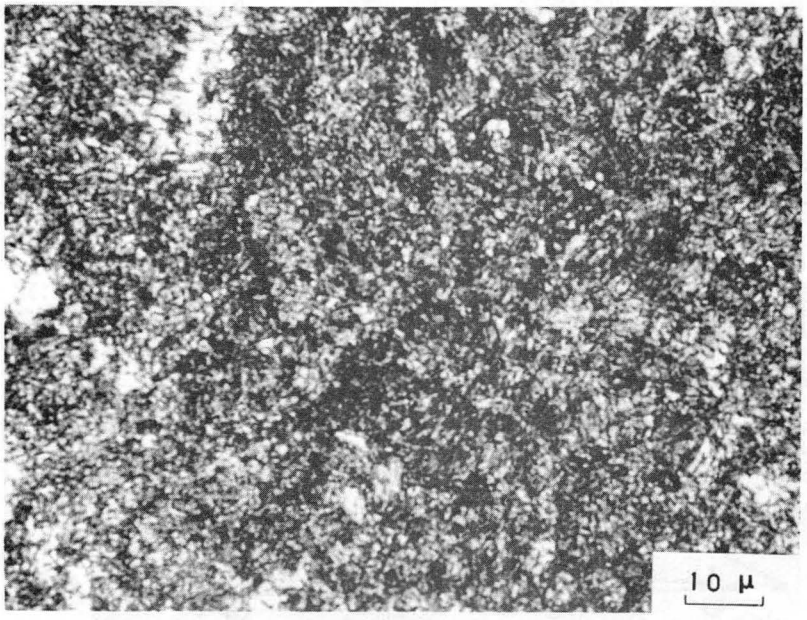

XBB 7411-7590

Fig. 2

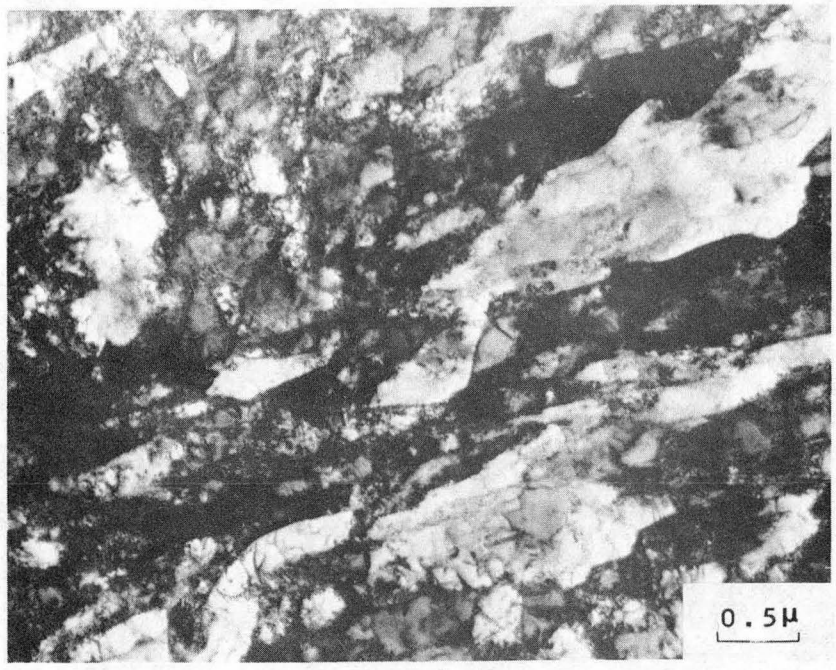

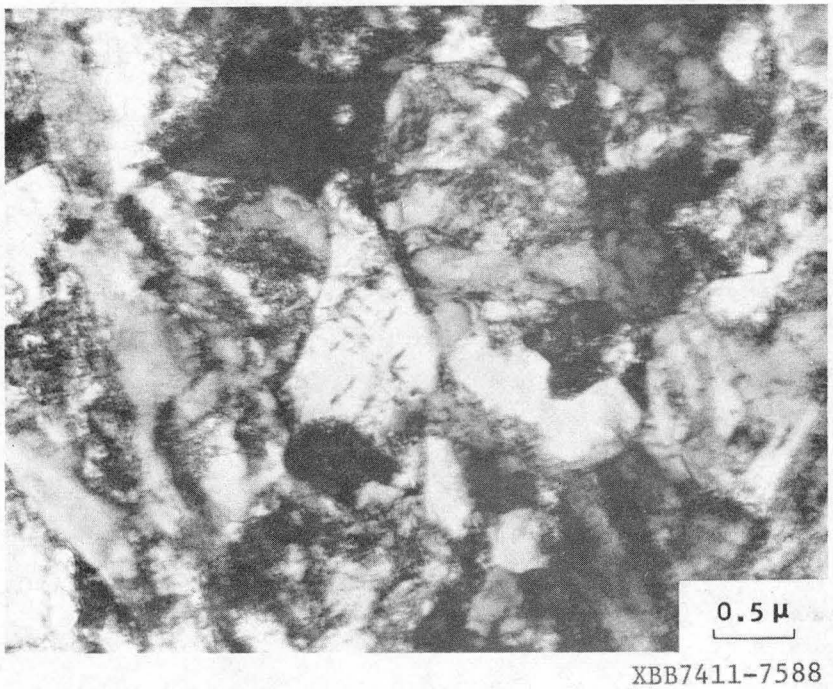

XBB7411-7588

Fig. 3

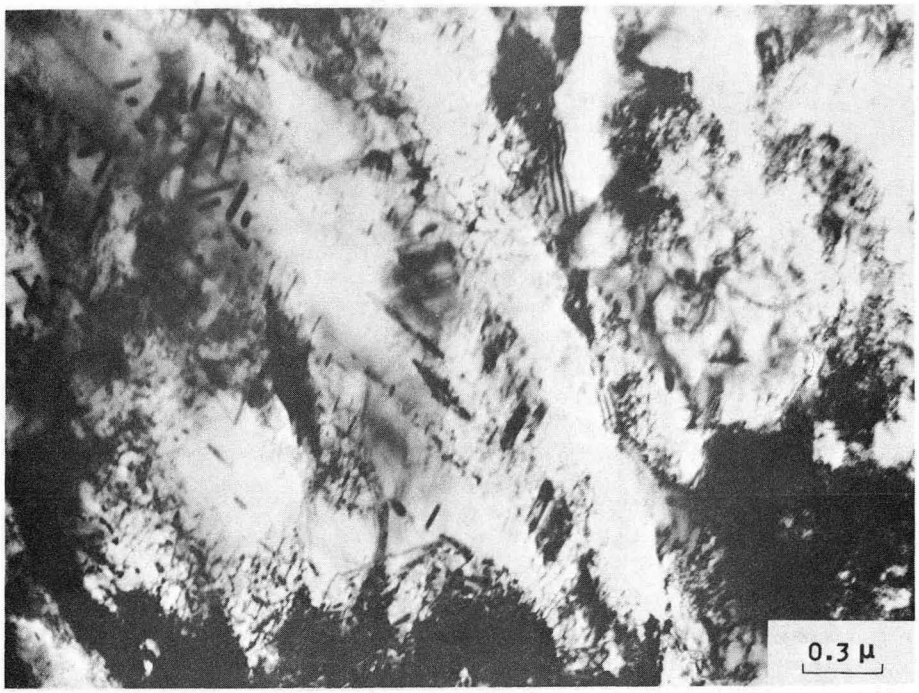

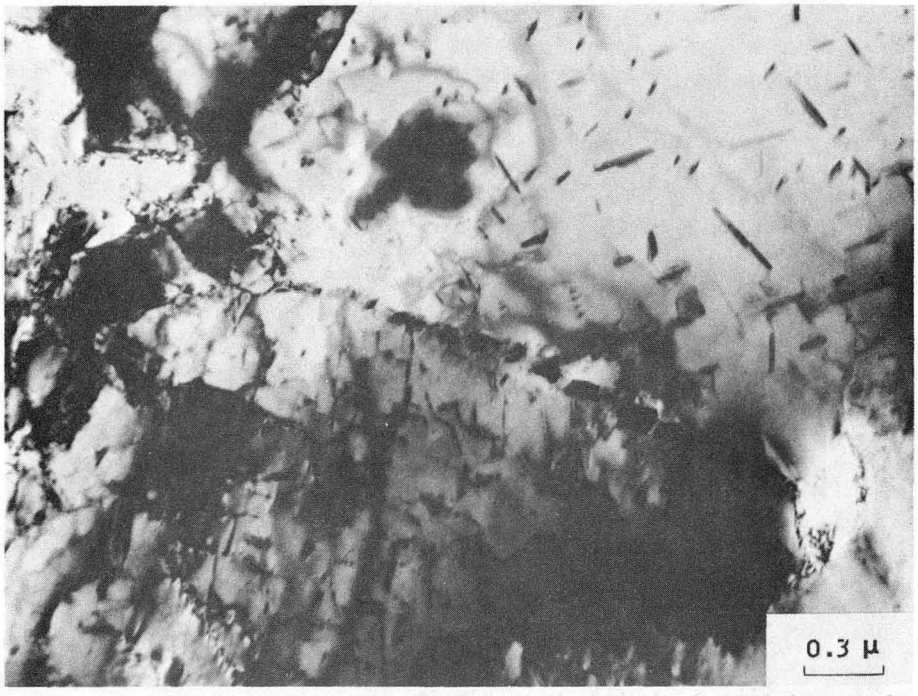

XBB7411-7587

Fig. 4

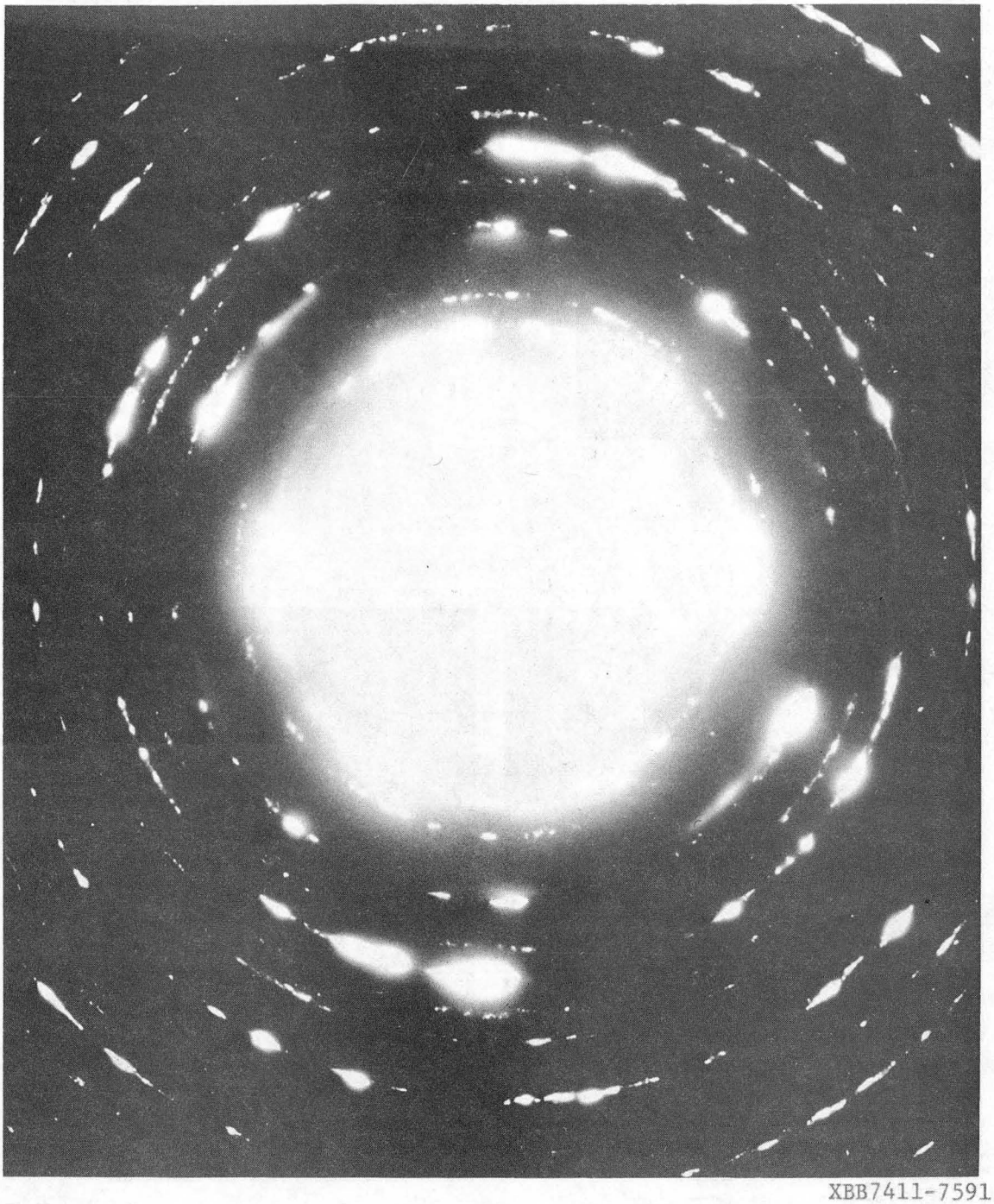

XBB7411-7591

Fig. 5

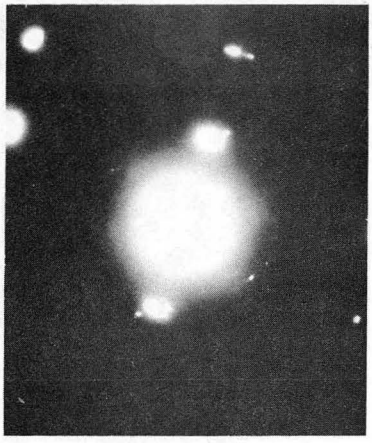

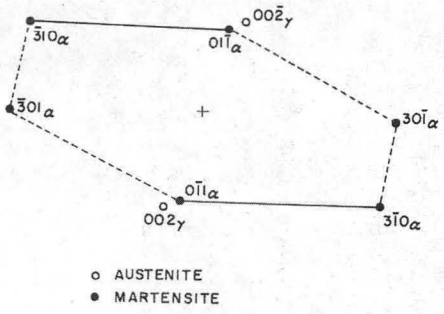

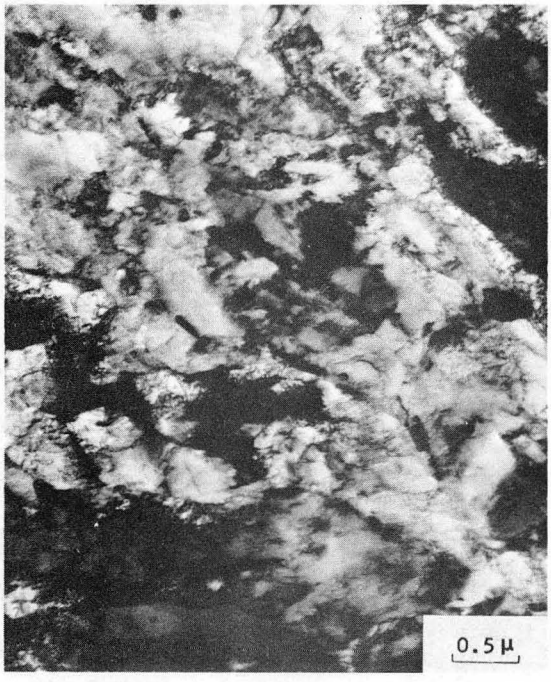

XBB 7411-7594

Fig. 6

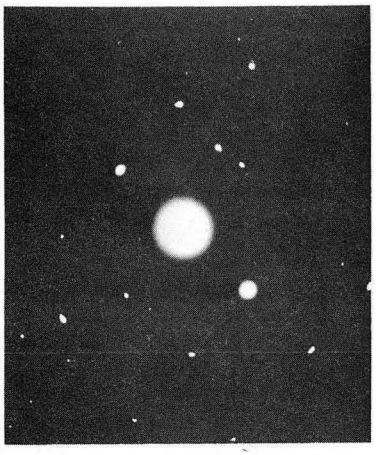

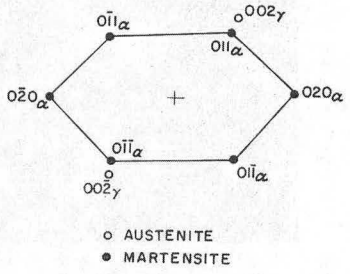

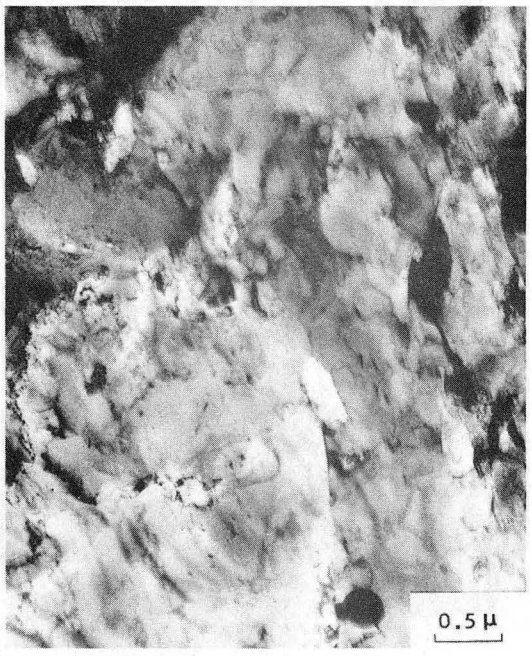

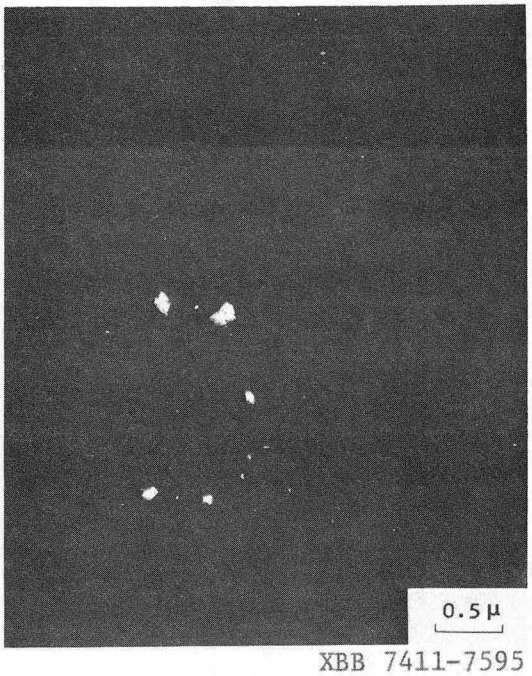

XBB 7411-7595

Fig. 7

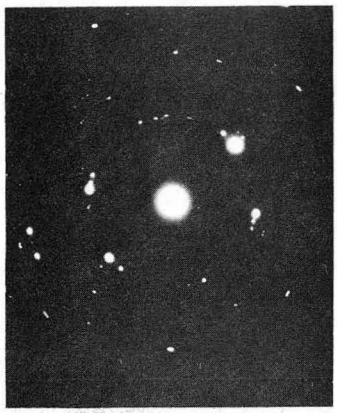

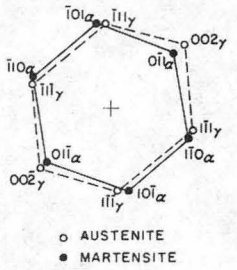

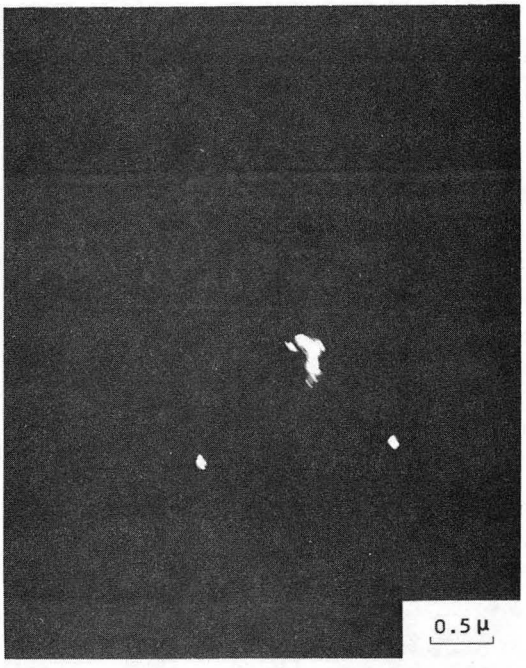

XBB 7411-7593

Fig. 8

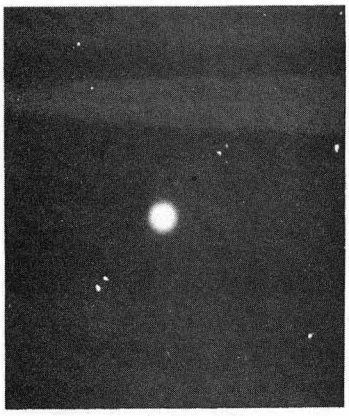

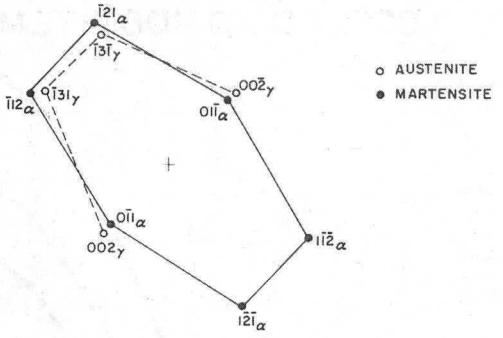

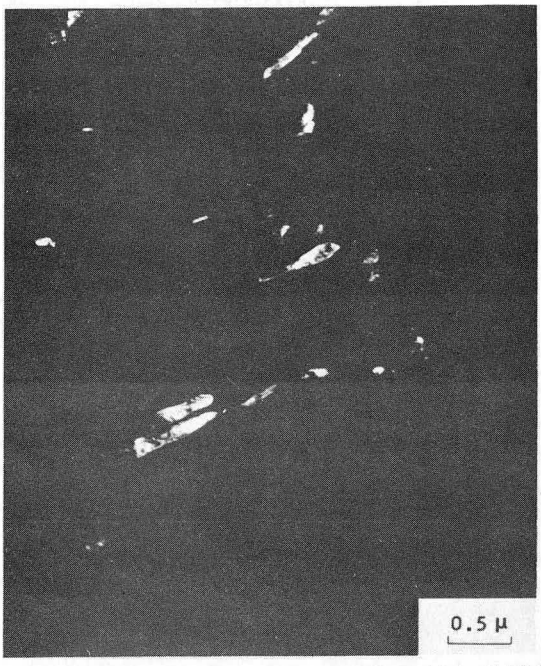

XBB 7411-7592

Fig. 9

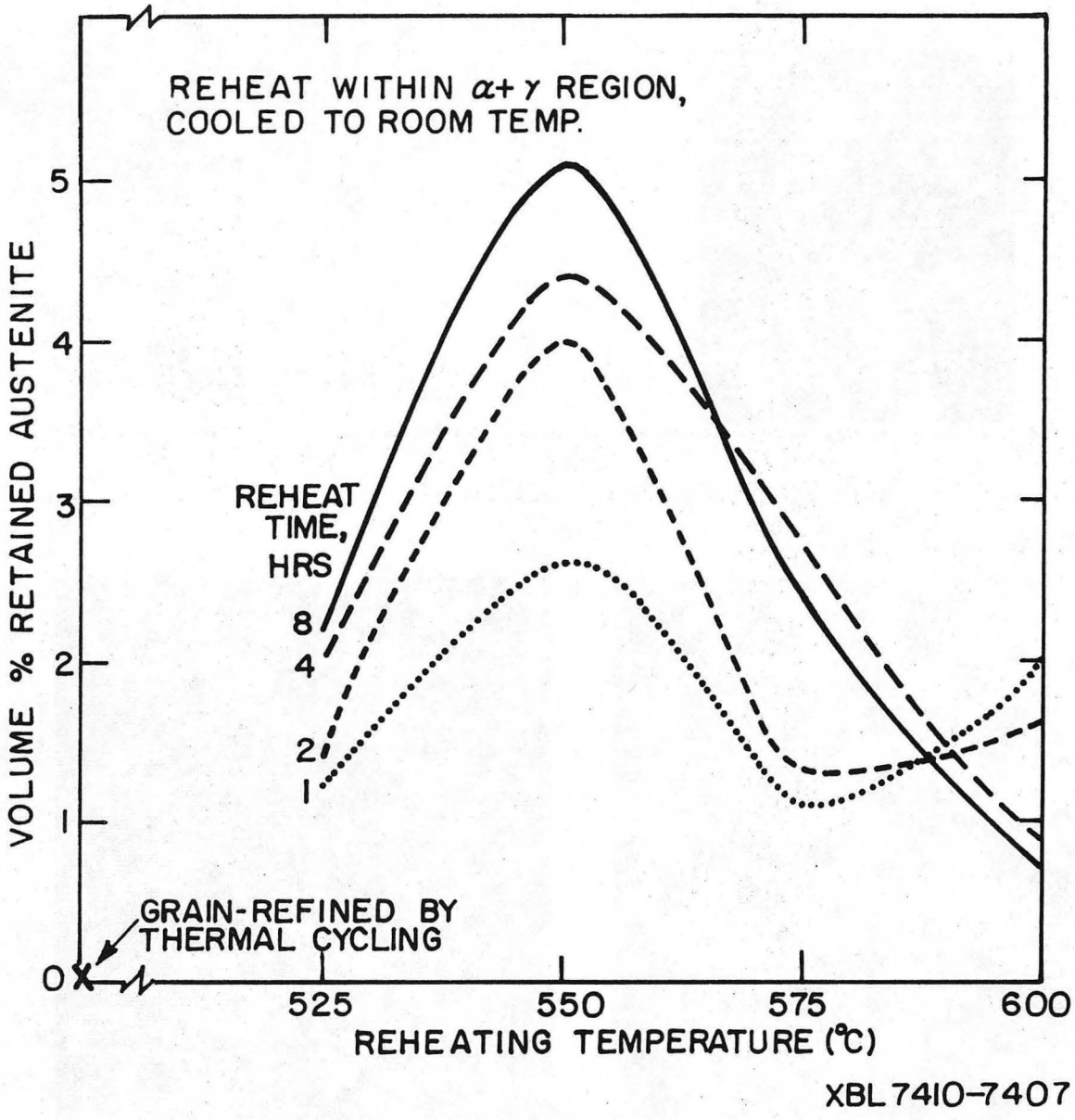
REHEAT WITHIN α+γ REGION,
COOLED TO ROOM TEMP.
VOLUME % RETAINED AUSTENITE
REHEAT TIME, HRS
8
4
2
1
GRAIN-REFINED BY THERMAL CYCLING
0
1
2
3
4
5
525
550
575
600
REHEATING TEMPERATURE (°C)
XBL 7410-7407

Fig. 10

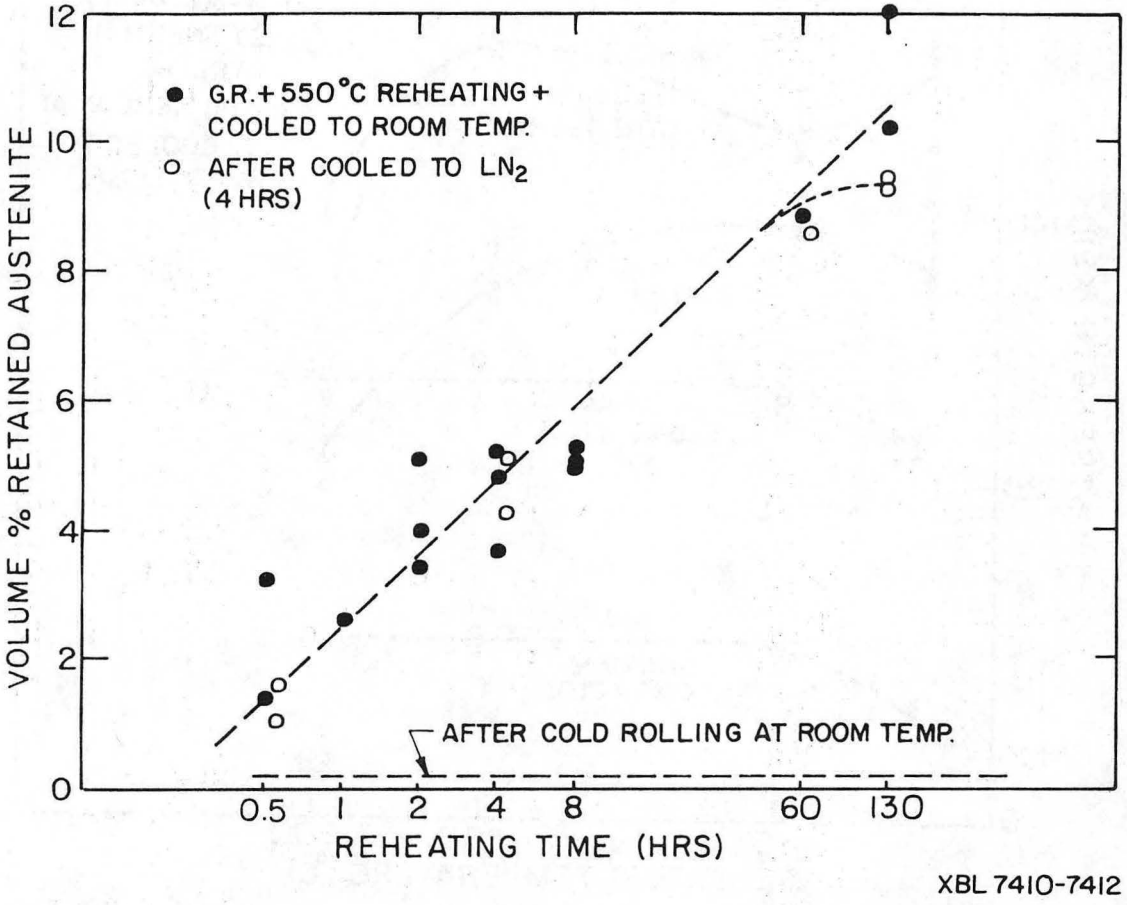

Fig. 11

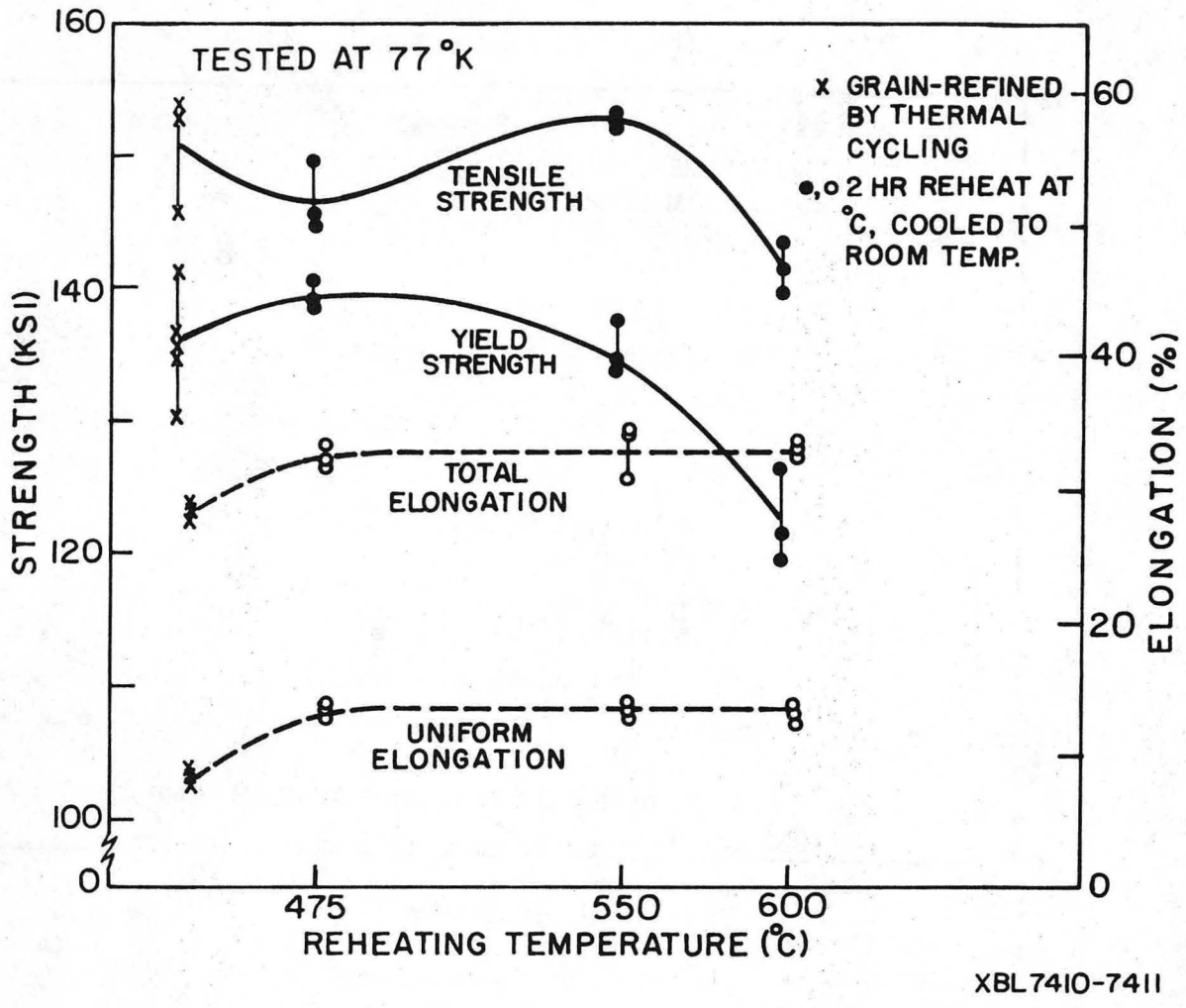
TESTED AT 77 °K
x GRAIN-REFINED BY THERMAL CYCLING
●,○ 2 HR REHEAT AT °C, COOLED TO ROOM TEMP.
TENSILE STRENGTH
YIELD STRENGTH
TOTAL ELONGATION
UNIFORM ELONGATION
STRENGTH (KSI)
ELONGATION (%)
160
140
120
100
0
60
40
20
0
475
550
600
REHEATING TEMPERATURE (°C)
XBL7410-7411

Fig. 12

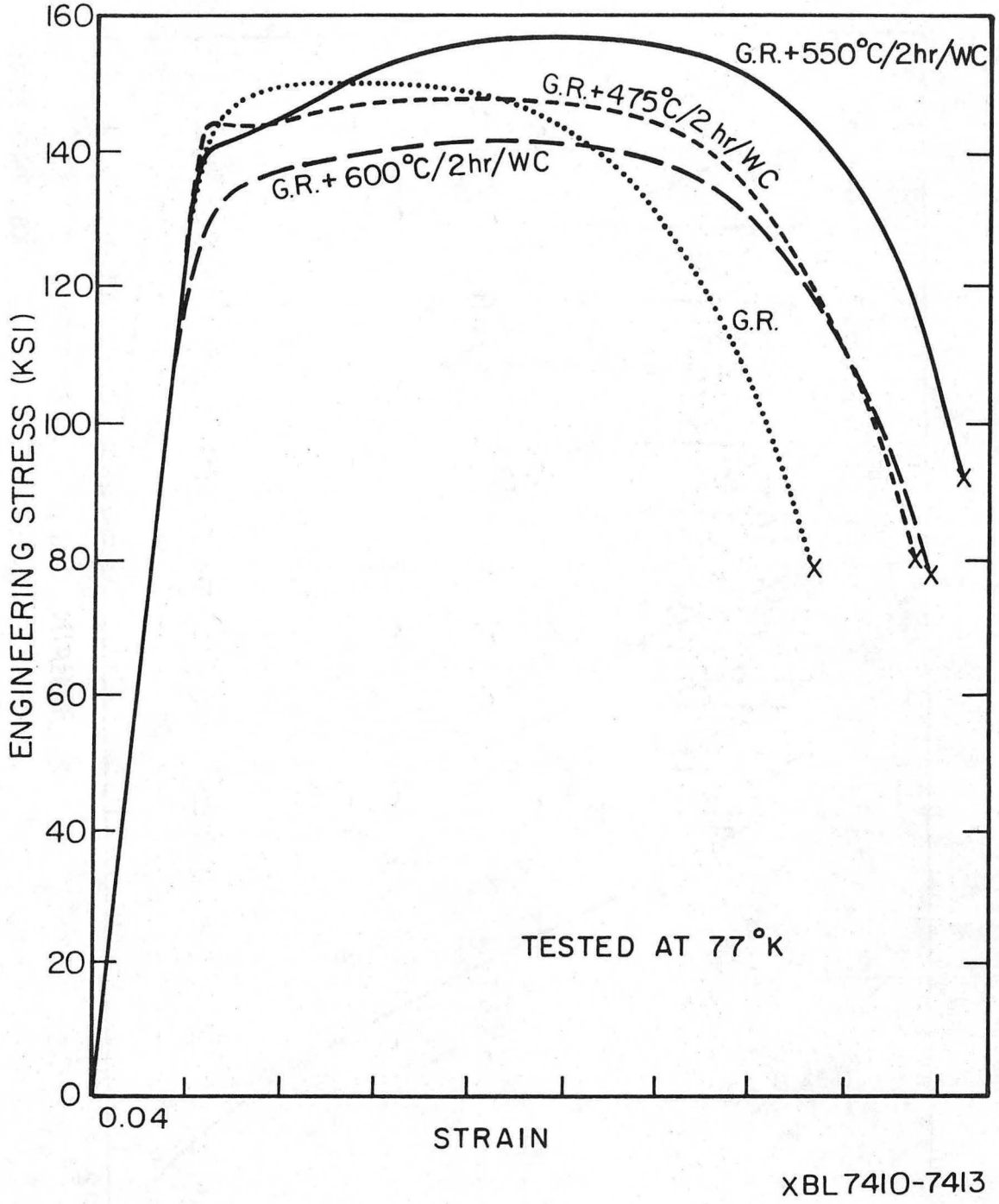

Fig. 13

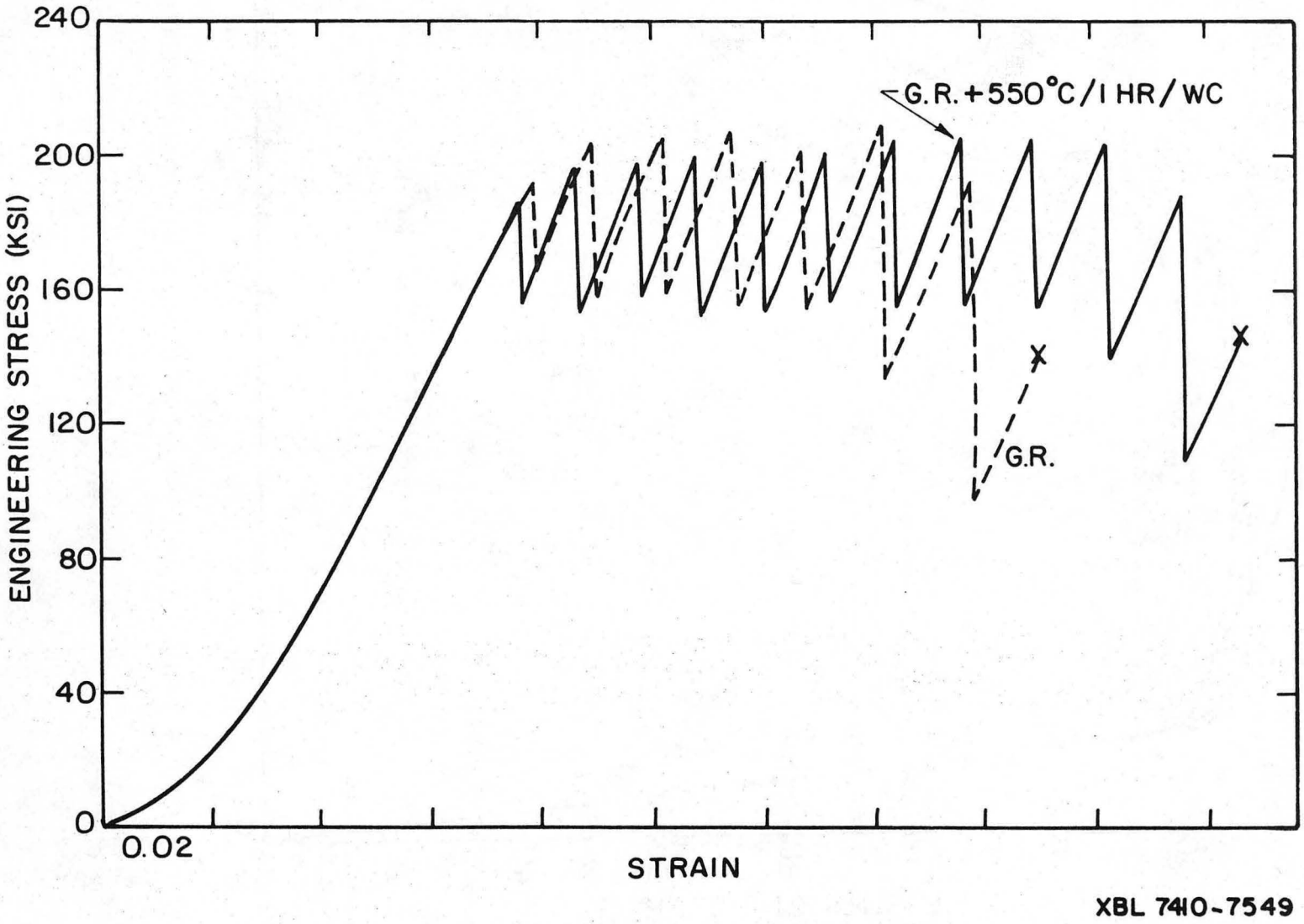
240
200
160
120
80
40
0
ENGINEERING STRESS (KSI)
0.02
STRAIN
G.R. + 550°C / 1 HR / WC
G.R.
XBL 7410-7549

Fig. 14

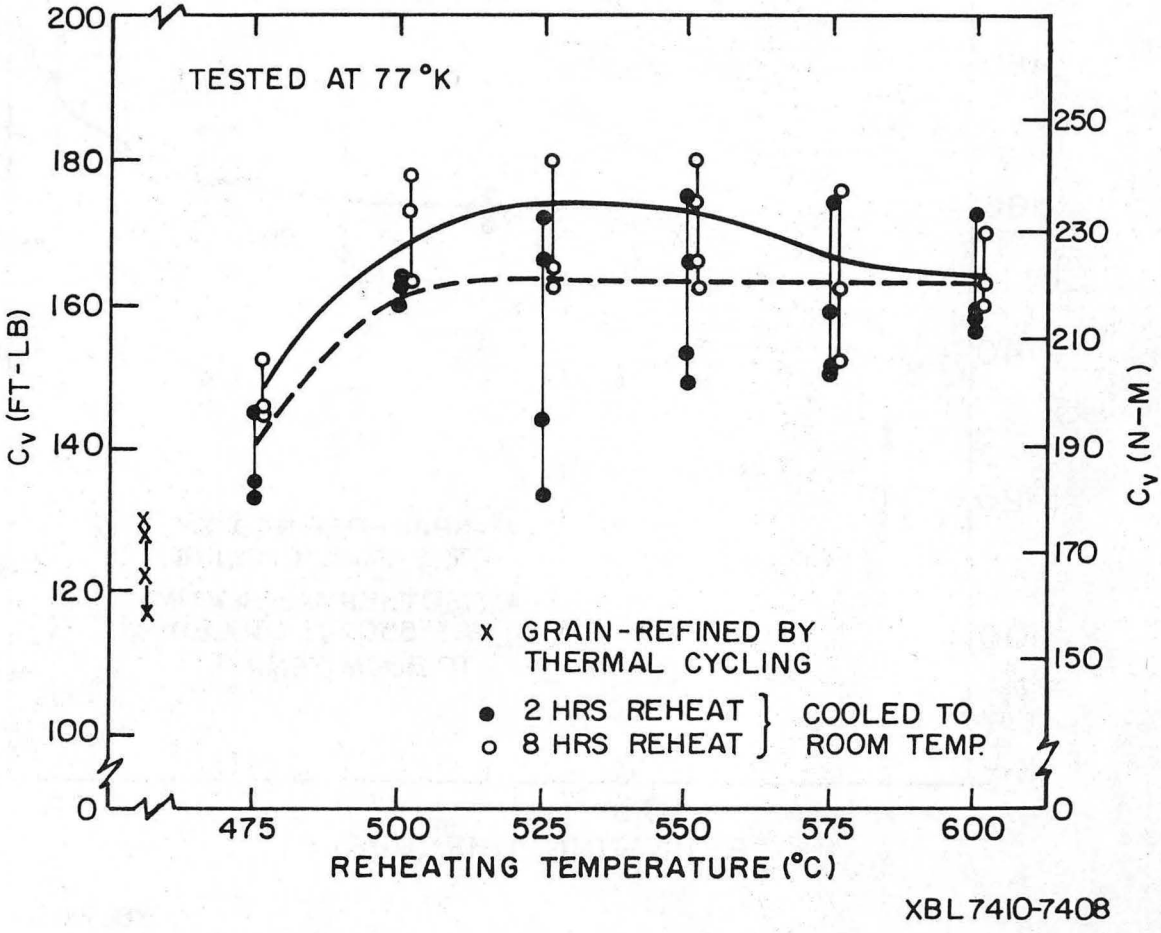

Fig. 15

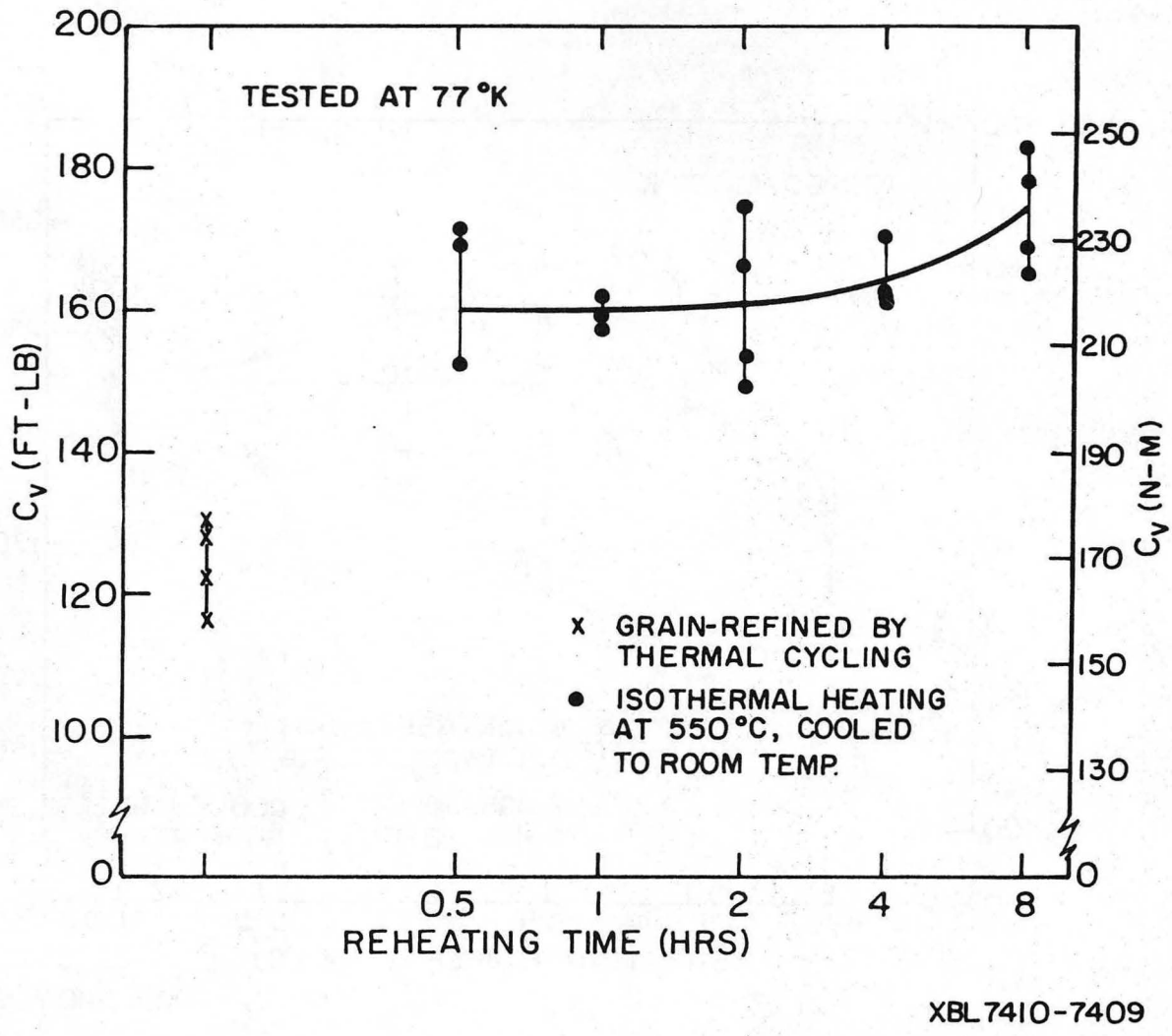
TESTED AT 77°K
200
180
160
140
120
100
0
250
230
210
190
170
150
130
0
C_V (FT-LB)
C_V (N-M)
x GRAIN-REFINED BY THERMAL CYCLING
● ISOTHERMAL HEATING AT 550°C, COOLED TO ROOM TEMP.
0.5
1
2
4
8
REHEATING TIME (HRS)
XBL7410-7409

Fig. 16

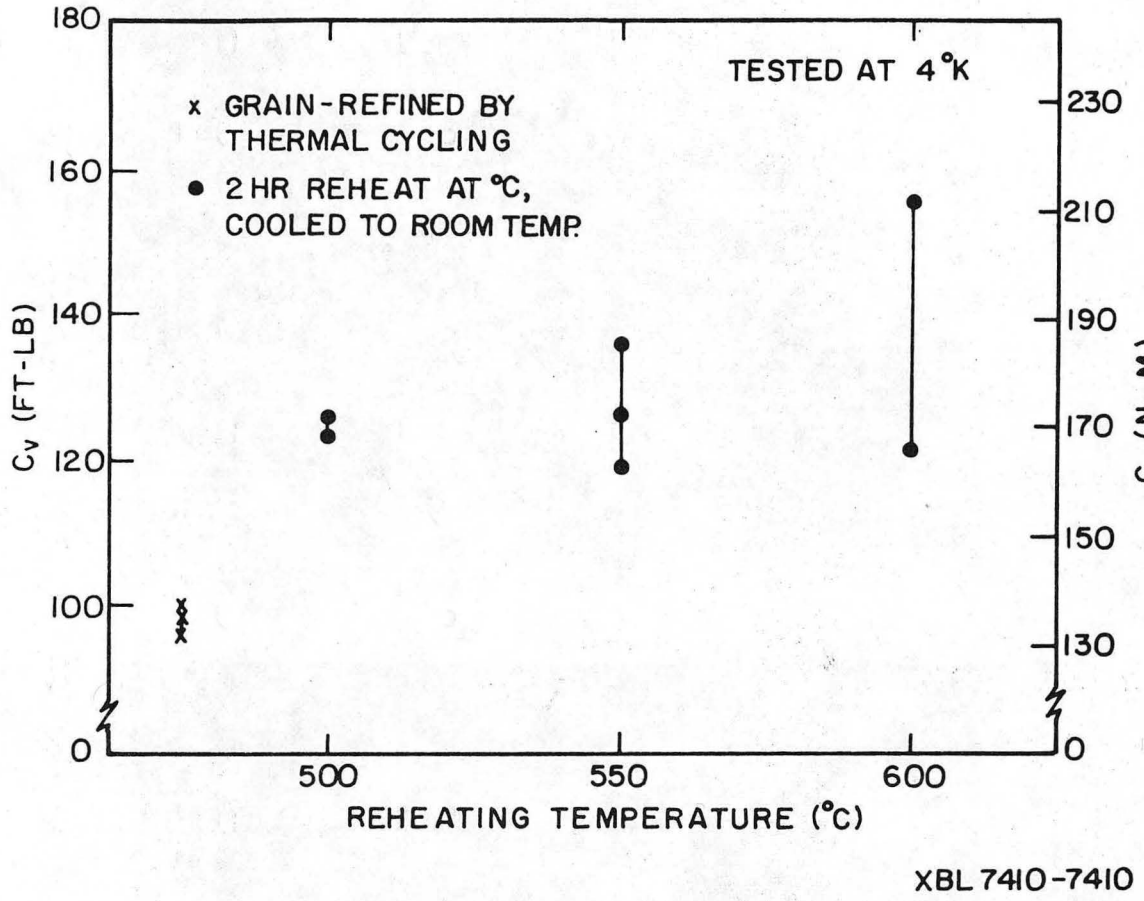

Fig. 17

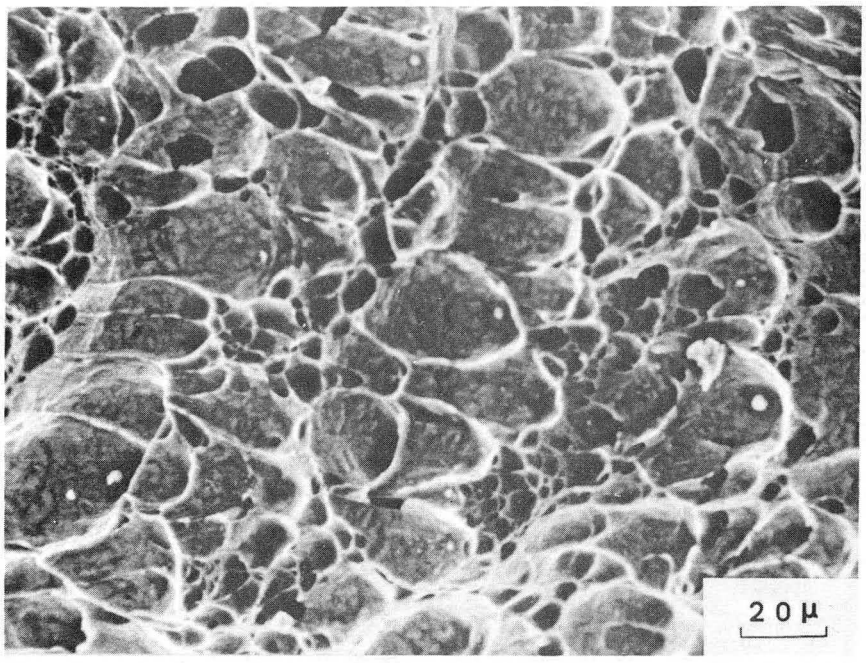

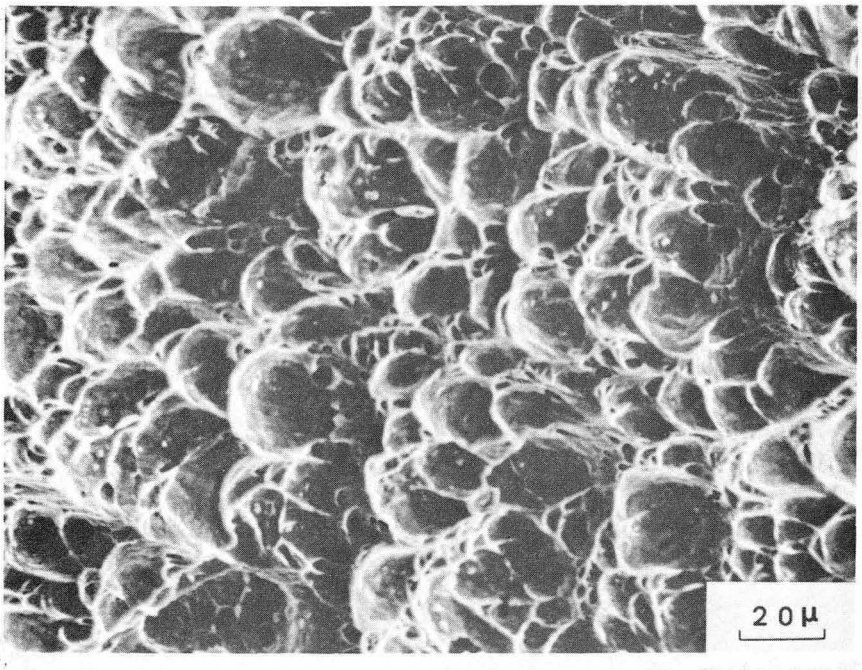

XBB 7411-7589

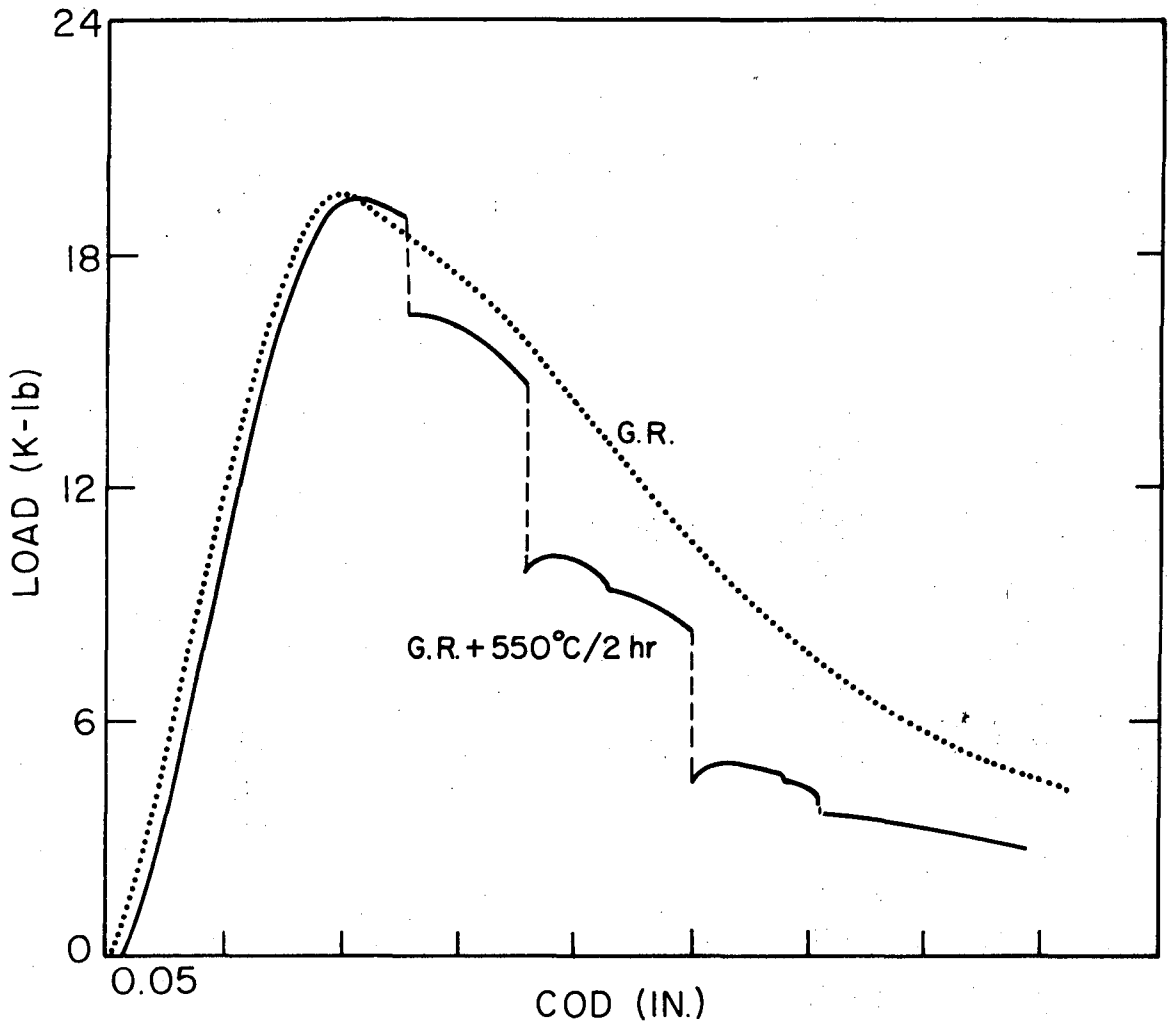

Fig. 19

TECHNICAL INFORMATION DIVISION
LAWRENCE BERKELEY LABORATORY
UNIVERSITY OF CALIFORNIA
BERKELEY, CALIFORNIA 94720